World Academy of Science, Engineering and Technology
International Journal of Aerospace and Mechanical Engineering
Vol:17, No:1, 2023

Effects of Boundary Conditions on the Dynamic Values of Solid Structures

F. Kadioglu, M. Z. Polat, A. R. Gunay

***Abstract*—**Correct measurement of a structural damping value is an important issue for the reliable design of the components exposed to vibratory and noise conditions. As far as a vibrating beam technique is concerned, the specimens under the test somehow are interacted with measuring and exciting devices, and also with boundary conditions of the test set-up. The aim of this study is to propose a vibrating beam method that offers a non-contact dynamic measurement of solid beam specimens. To evaluate the possible effects of the clamped portion of the specimens with clamped-free ends on the dynamic values (damping and the elastic modulus), the same measuring devices were used, and the results were compared to those with the free-free ends. First, the governing equations of beam specimens related to the free-free and clamped-free boundary conditions were expressed to be able to find their natural frequencies, flexural modulus and damping values. To get a clear idea of the sensitivity of the boundary conditions to the damping values at low, medium and high levels, representative materials were subjected to the tests. The results show that the specimens with low damping values are especially sensitive to the boundary conditions and that the most reliable structural damping values are obtained for the specimens with free-free ends. For the damping values at the low levels, a deviation of about 368% was obtained between the specimens with free-free and clamped-free ends, yet, for those having high inherent damping values, comparable results were obtained. It was obvious that the set-up with clamped-free boundary conditions was not able to produce correct/reliable damping values for the specimens with low inherent damping.

***Keywords*—**Boundary conditions, damping, dynamic values, non-contact measuring systems, vibrating beam technique.

I. Introduction

AERIAL and ground vehicles are subjected to vibratory conditions during their service life, resulting in fatigue, noise, comfort and health problems that are not desired by the designers. A remedy to overcome these problems is to use components with high structural damping in these vehicles. There have been many efforts to increase the damping values in the structures. For example, Prabhakaran et al. [1] investigated vibration and sound absorption damping capabilities of flax fiber reinforced composites and compared them with glass fiber reinforced composites. The experimental results suggested that the flax fiber reinforced composites could be a viable candidate for applications that need good sound and vibration properties. Sargianis et al. [2] explored and characterized the sound and vibration damping properties of natural material-based sandwich composites. It was experimentally observed that using a natural fiber-based face sheet with a balsa wood core led a 100% improvement in coincidence frequency and acoustic performance, and also a combination of synthetic core with the natural fiber-based face sheet exhibited a 233% increase, compared to fully synthetic sandwich composite. Jeyaraj et al. [3], [4] investigated the vibration and acoustic response of a composite plate and visco-elastic sandwich plate with inherent material damping in a thermally controlled environment. Results say that resonant amplitudes of vibration and acoustic response are reduced by the inherent damping. Arunkumar et al. [5] analyzed the vibro-acoustic response of honeycomb core sandwich panels with composite facings and showed that the inherent damping associated with composite facing significantly increases the sound transmission loss while reducing resonant amplitudes. Petrone et al. [6] calculated experimentally the radiated acoustic power from the aluminum foam sandwich panel. Petrone et al. [7] attained an improvement in damping value by filling the wool fiber in the core, thereby achieving better acoustic performance in eco-friendly honeycomb cores for sandwich panels.

It has shown been that the inherent damping in materials has a positive impact on their fatigue life [8], [9]. From the efforts mentioned above, it is obvious that correct damping measurements of the structures are a vital issue for a reliable design. Therefore, when a sample of the relevant structures is subjected to experimental tests, all precautions must be taken as the test set-up has important effects on the measured values. As far as a vibrating beam test is concerned, a specimen under the test is quite likely to interact with measuring and exciting devices, and also with end conditions that bear the possibility of extraneous damping values. There have been many works in the literature related to such experiments, but a specific emphasis has not been made on the values of possible extraneous damping. For example, Attard et al. [10] conducted a series of vibration tests to quantify the damping properties of composite beams, either as self-standing composite laminates or as retrofitting materials for structural substrates. The specimens were supported horizontally in clamped-clamped end conditions, and a laser vibrometer was used to measure the velocity-time histories of the test beams. Forced vibration tests were performed using an electromagnetic shaker. Banded white noise excitations with peak acceleration amplitudes of 0.0003

F. Kadioglu is with the Department of Aerospace Engineering, Ankara Yildirim Beyazit University, Ankara, 06050, Turkey (e-mail: fkadioglu@ybu.edu.tr).

M. Z. Polat works as a Research Assistant at Yıldırım Beyazıt University and continues his master's degree at Yildirim Beyazit University, Ankara, 06050, Turkey.

A. R. Gunay is the Division manager of Construction Maintenance Operating Division at TUBITAK SAGE. He also works as a part-time employee at Atılım University, Mamak, Ankara, 06261, Turkey (e-mail: reha.gunay@tubitak.gov.tr).

kg and 0.003 kg were used to excite the beam specimens. Two accelerometers were mounted on the shaker base to ensure that the actual excitation signal complied with the desired input signal. Rafiee et al. [11] used a vibrating beam technique to measure the natural frequencies and damping factors of nanocomposite specimens in the form of cantilever beams. The clamped-free beam was excited by a vibration shaker at the clamped end, and the response of the beam was tracked by means of accelerometers and the computed frequency response functions (FRFs) gave information about the natural frequencies of the composite beams.

To study the vibration behavior of the composite and sandwich beams, free vibration tests were carried out by Monti et al. [12]. The beams were tested in a clamped-free configuration and excited by an impact hammer close to the clamped end. The displacement of the free end was measured by a laser vibrometer. The experiment set-up created by Sargianis and Suhr [13] involved a beam with clamped–clamped end conditions. An electrodynamic shaker with an impedance head attached to it to measure the input force was excited with a random noise signal ranging from 20 to 4000 Hz. A micro-accelerometer with a mass of 0.0006 kg was used to measure the FRF at the equidistant points along the beams. In another work [14], an experimental set-up included an excitation force applied centrally on the plate via an electromagnetic shaker attached to the plate using glue, and an accelerometer glued to the surface of the plate to record the response. Arunkumar et al. [15] used an electrodynamic shaker to vibrate a honeycomb structure fixed at the bottom in the center by a clamping system, and an accelerometer mounted on the honeycomb structure to get the response. In another work, beam specimens from the CFRP (Carbon-fiber-reinforced polymers) laminates and nanocomposite plates were tested in both the free vibration and forced vibration. In the free vibration test, the specimens with clamped-free end conditions were used, while the free end was deflected as a certain displacement before release. A digital storage cathode ray oscilloscope was used to store the vibration response's data, which was continuously monitored using the accelerometer attached to the specimen's tip [16]. A modal analysis was carried out using an experimental test set incorporating the specimens with clamped-free ends. The specimens were vibrated by giving the excitation using an impact hammer, and the response was obtained using an accelerometer [17]. A dynamic mechanical analysis was performed on composite specimens to provide a clamp-free measurement using a non-resonant damping experiment. Also, vibration beam measurements were conducted to allow the measurement of resonant damping at very large amplitudes, identify many modes of vibration and study a broad frequency range. The test was performed on the clamped-free beams with a pre-defined deflection and the response was obtained with a laser displacement sensor. Accelerometers were mounted to the free edge and to the shaker for controlling purposes [18].

For another test, a strain gauge was glued on the specimen vibrated with a shaker and connected with the data acquisition system to receive data [19]. More references can be given [20]-[25] for similar experiments but one common conclusion coming out is clear; all the instruments attached to the specimens are likely to affect the dynamic values. Namely, any exciting and/or measuring devices such as accelerometers, shakers and strain gauges attached to the specimens under the vibration test are believed to contribute to the measured damping values. Similar situations would be the case for the specimens with fixed (clamped) ends. Despite this fact, any study on the specimens with a non-contact measuring device, and also with free-free ends is only a few in the literature.

The aim of this study is to propose an experimental set-up to be able to measure reliable damping values of specimens subjected to a vibrating beam technique. For this purpose, first, the specimens with free-free ends were vibrated using non-contact measuring and exciting test devices to make sure that the specimens were isolated as much as possible. Then, with the same experimental devices, the same specimens were tested using clamped-free end conditions to evaluate any potential extraneous damping value in the clamped part. The specimens were classified into three different categories to see the impact of the extraneous values on the structural damping of the specimens: category1- those with low structural damping values, category2- those with medium values, and category3- those with high values. The analytical formulations as well as solutions relevant to the boundary conditions have also been presented to calculate the dynamic values (damping and flexural modulus) of the specimens used.

II. Experimental Works

A. The Materials and Specimens Used

To be able to see the sensitivity of the specimen's damping value to the boundary conditions and the two test techniques, the specimens were classified into three different categories which can be seen in Fig. 1; category1- the Specific Damping Capacity (SDC) values up to 2%, called the specimens with low damping, category2- the SDC values between 2% and 5.5%, called those with medium damping, and category3- the SDC values above 5.5%, called those with high damping. It is important to note that the set-up with free-free boundary conditions was considered for this classification as this set-up was found more reliable compared to that with clamped-free boundary conditions, especially the case for measuring the specimens with low damping values. For this purpose, the specimens were manufactured from three different materials, a 2024-T3 aluminum alloy, a glass fiber-reinforced polymer matrix composite, and a carbon fiber-reinforced epoxy matrix composite. For the specimens with low damping category, the 2024-T3 aluminum alloy (Al), the glass fiber-reinforced prepregs with longitudinal (0°) directions (GFL), and the woven carbon fiber-reinforced prepregs with longitudinal directions (CFL) were selected. While for those with medium damping category, the glass fiber-reinforced prepregs with ± 10° (GF10), ± 20° (GF20, and ± 35 (GF35), for those with high damping category the glass fiber-reinforced prepregs with ± 45° (GF45), ± 80° (GF80), and the woven carbon fiber-reinforced prepregs with ± 45° (CF45) were selected. For the glass fiber-reinforced

specimens, the composite plates with 10 layers, Hexply 913/33%/UD280, produced by Hexcel, were cured according to the manufacturer's datasheet, at 130 °C for 120 minutes under a pressure of 5 bars, and machined to the required dimensions of beams. For the carbon fiber-reinforced specimens, the beam manufactured from a prepreg of woven carbon fiber-reinforced epoxy matrix composite, Hexply 8552S/A280-5H, produced by Hexcel, is cured at 120 °C for 120 minutes, after an initial heating-up procedure of 80 °C for 90 minutes under a pressure of 5 bars.

The specimens were machined from the plates, and the details of the specimens for the vibration test are shown in Table I. All the tests were carried out under a controlled environment, at room temperature (23 °C) and 50% relative humidity, to avoid environmental effects on the specimens, and four specimens of each type were tested to see if the results were repeatable.

B. The Experimental Set-up with Free-Free End Conditions

A detail about the two-dimensional (2-D) vibrating beam test set-up with a configuration of free-free ends is shown in Fig. 2. It is seen from the test that an electromagnetic shaker connected to the power amplifier is used to produce sinusoidal motion. The response from the beam is detected via a laser doppler (laser head) placed above the specimen. The input and output signals together are connected to an oscilloscope to observe the resonant frequency at which all measurements are made. In vibrating the specimens, a non-contact mechanism was aimed, which has been detailed in the three- dimensional (3-D) test set-up, Fig. 3. For this purpose, a thin plate with an area of 4.6 cm^2 was glued to the top of the shaker, and when it was vibrated, the plate could produce a sinusoidal-induced air flow and vibrate the specimens. Since there is no direct contact between the shaker and the specimen during excitation, or between the sample and the laser head during response acquisition, such a mechanism is believed to provide an accurate measurement of material damping. In this way, it was possible to isolate the specimens from the measuring and exciting devices that were parts of the experimental set-up. It is also important to note that the specimen under the test should be placed at the exact nodal positions which are crucial for the correct measurements, too. For the current study, all the measurements were made at the first (fundamental) natural frequency, so the first mode shape and this case, the specimen beams with length l were placed on the ropes connected to the U-shaped mobile supports shown in Fig. 3. For the first mode, 0.224l of the beams were placed at the theoretical nodal positions, distances from the free ends.

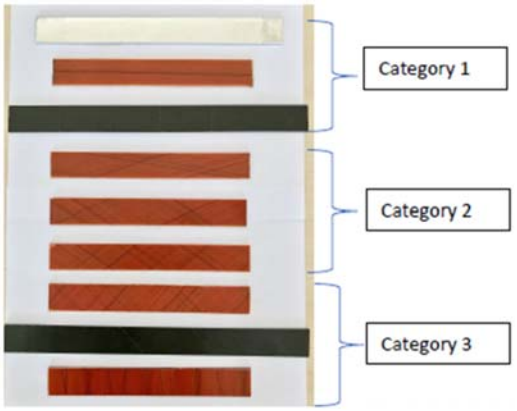

Fig. 1 A representative of specimens from each category used for the vibration tests

TABLE I
THE DETAILS OF THE SPECIMENS USED FOR THE DYNAMIC EXPERIMENTAL WORK

Specimens	Width (mm)	Thickness (mm)	Length (mm)	Mass (g)	Density (kg/m^3)
Al	26.10	1.97	250.0	35.42	2755.50
CFL	25.37	2.31	301.0	27.22	1543.10
GFL	25.44	1.909	202.8	17.70	1797.46
GF10	24.98	1.873	200.4	16.68	1778.91
GF20	24.97	1.842	196.5	16.24	1796.58
GF35	24.89	1.853	200.1	16.52	1789.72
CF45	25.60	2.32	301.5	27.28	1523.45
GF45	25.64	1.937	200.5	17.62	1769.14
GF80	25.65	1.958	199.4	17.50	1747.68

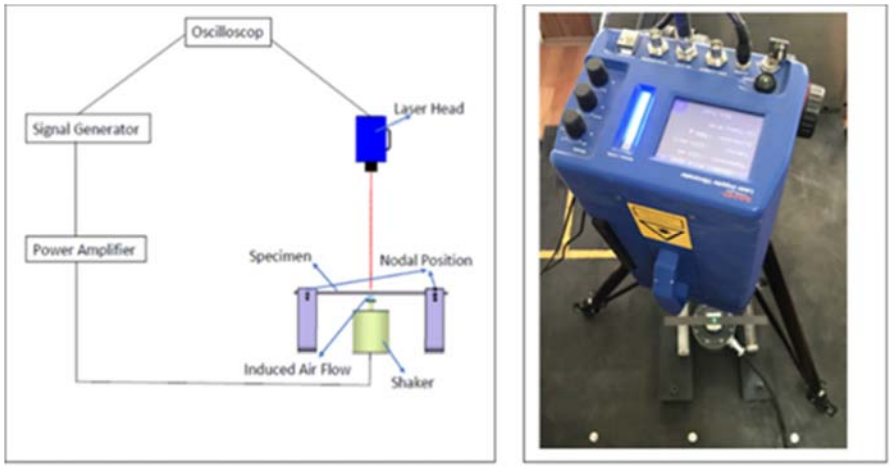

Fig. 2 A representative 2-D illustration of the vibrating beam test with free-free end conditions

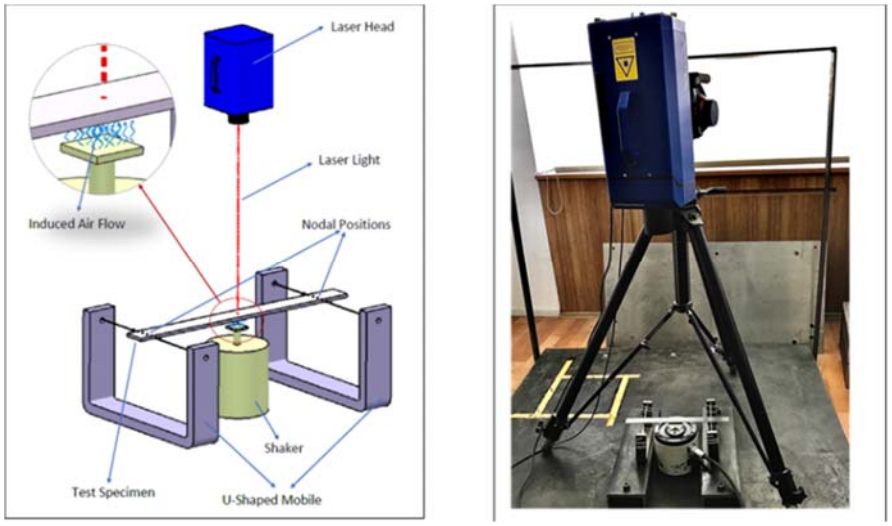

Fig. 3 A representative detailed 3-D illustration of the vibrating beam test with free-free end conditions

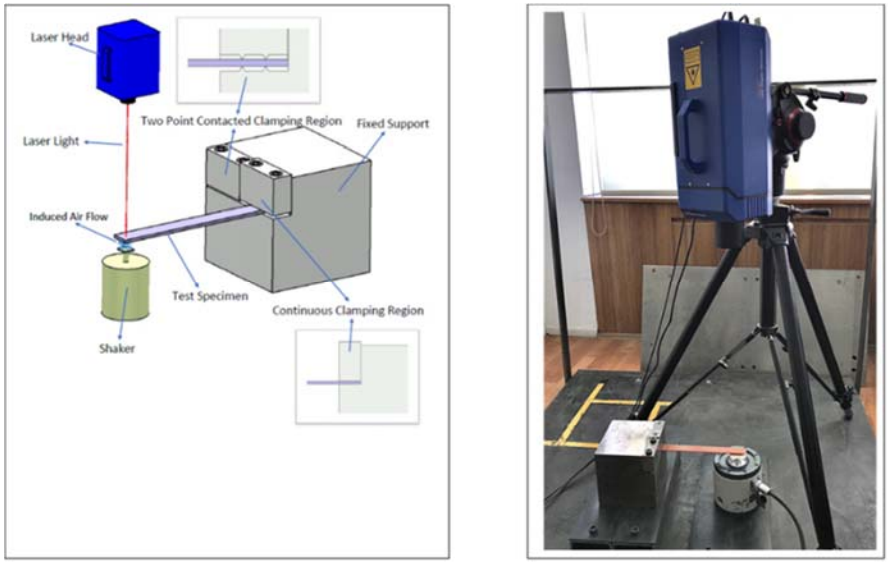

Fig. 4 A representative 3-D illustration of the vibrating beam test with clamped-free end conditions

C. The Experimental Set-up with Clamped-free End Conditions

The experimental set-up for the specimens with clamped-free boundary conditions is shown in Fig. 4.

The same measuring and exciting devices (with non-contact mechanisms) were used for those with free-free ends. The main reason to conduct this test is to be able to evaluate the potential extraneous damping value from the clamping part of the specimen. As indicated in Fig. 4, two different types of the clamping region were prepared to get a better insight; 1- a 28 mm-continuous clamping region where there was a constant interaction of fixed support with the specimen's clamped part, and 2- a clamping region with two-contact points where there were two different points of interactions of the fixed support with the specimen's clamped part. It is important to note that the specimens subjected to the vibration tests were tightened firmly in the clamping region to avoid any undesired effects and that the fixed support from the mild steel had enough weight to provide a viable clamped condition.

III. Theory

A. Flexural Vibration

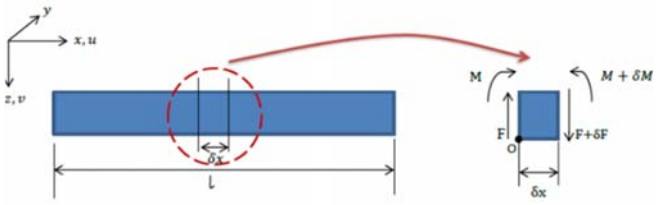

Fig. 5 Free-body diagram of an element of a beam subjected to flexural vibration

We consider the free-body diagram of an element of a beam with no external force, shown in Fig. 5 where M is the bending

moment and F is the shear force, which are length (x) and time (t) dependent.

The moment equation of motion about the y-axis passing through point O in Fig. 5 results in (1):

$$(F + \delta F)\delta x + (M + \delta M) - M = 0 \tag{1-a}$$

By ignoring $\delta \mathrm{F} \delta x$, the equation becomes;

$$\mathrm{F} = -\frac{\delta M}{\delta x} = -\frac{dM}{dx} \tag{1-b}$$

The force equation of motion of an element of a uniform beam in the z direction is: $\mathrm{F} + \delta \mathrm{F} - \mathrm{F} = mass\ x\ acceleration\ of\ mass$;

$$\delta \mathrm{F} = \rho A\ \delta x\ \frac{\partial^2 V}{\partial t^2} \tag{2-a}$$

where ρ is the mass density, A is the cross-sectional area of the uniform beam and v is the displacement in the z-direction. Remember, $\mathrm{F} = -\frac{dM}{dx}$, so,

$$\frac{d\mathrm{F}}{dx} = \frac{-\partial^2 M}{\partial x^2} \tag{2-b}$$

$$\text{and} \quad M = EI\frac{\partial^2 V}{\partial x^2} \tag{2-c}$$

$$\text{so,} \quad \frac{d\mathrm{F}}{dx} = -EI\frac{\partial^4 V}{\partial \mathrm{x}^4} \tag{2-d}$$

So, the differential equation of the motion is;

$$-EI\frac{\partial^4 V}{\partial x^4} = \rho A\frac{\partial^2 V}{\partial t^2} \tag{3}$$

where E is Young's modulus and I is the moment of inertia of the beam cross-section about the z-axis.

The solution to (3) is: $v = (P\cos(\alpha x) + Q\sin(\alpha x) + R\cosh(\alpha x) + S\sinh(\alpha x))(T\cos(wt) + U\sin(wt))$ where P, Q, R, S, T and U are constants that can be obtained from the boundary and initial conditions, while ω is the natural frequency of vibration, and α is known as the normal mode or characteristic function of the beam having infinite numbers of the modes. The value of α can be determined from the boundary conditions of the beam.

It can be proved that:

$$\frac{\partial^4 v}{\partial x^4} = \alpha^4(P\cos(\alpha x) + Q\sin(\alpha x) + R\cosh(\alpha x) + S\sinh(\alpha x))(T\cos(\omega t) + U\sin(\omega t)) \tag{4}$$

$$\text{so,} \ \frac{\partial^4 v}{\partial x^4} = \alpha^4 v \tag{5}$$

and,

$$\frac{\partial^2 V}{\partial t^2} = (P\cos(\alpha x) + Q\sin(\alpha x) + R\cosh(\alpha x) + S\sinh(\alpha x))\omega^2(-T\cos(\omega t) - U\sin(\omega t))$$

so,

$$\frac{\partial^2 v}{\partial t^2} = -\omega^2 v \tag{6}$$

$$-EI\alpha^4 V = -\rho A\omega^2 v, \text{ so,} \quad \alpha^4 = \frac{\rho A\omega^2}{EI} \tag{7}$$

Because the equations of motion involve second-order derivative with respect to time and fourth-order derivative with respect to x, two initial conditions and four boundary conditions are required to find a unique solution for displacement in the z-direction.

For a beam with free-free boundary conditions, at $x = 0$, and at $x = l$, the bending moment (BM) and the shear force (SF) are equal to zero, thus;

$$BM = EI\frac{\partial^2 \mathrm{F}}{\partial x^2} = 0, \ \text{or} \ \frac{\partial^2 \mathrm{F}}{\partial x^2} = 0 \tag{8}$$

$$SF = -EI\frac{\partial^3 \mathrm{F}}{\partial x^3} = 0, \ \text{or} \ \frac{\partial^3 \mathrm{F}}{\partial x^3} = 0 \tag{9}$$

$$\frac{\partial^2 v}{\partial x^2} = \alpha^2(-P\cos(\alpha x) - Q\sin(\alpha x) + R\cosh(\alpha x) + S\sinh(\alpha x))(T\cos(\omega t) + U\sin(\omega t))$$

$$\frac{\partial^3 v}{\partial x^3} = \alpha^3(P\cos(\alpha x) - Q\sin(\alpha x) + R\cosh(\alpha x) + S\sinh(\alpha x))(T\cos(\omega t) + U\sin(\omega t))$$

Thus, for the boundary conditions at $x = 0$

$$0 = \alpha^2(-P + R), \text{ so,} \quad P{=}R \tag{10}$$

$$0 = \alpha^3(-Q + S), \text{ so,} \quad Q{=}S \tag{11}$$

Also, the boundary conditions at $x = l$ are as follows;

$$0 = \alpha^2(-P\cos(\alpha l) - Q\sin(\alpha l) + P\cosh(\alpha l) + Q\sinh(\alpha l)) \tag{12}$$

$$0 = \alpha^3(P\sin(\alpha l) - Q\cos(\alpha l)) + P\sinh(\alpha l) + Q\cosh(\alpha l) \tag{13}$$

$$P(\cos(\alpha l) - \cosh(\alpha l)) = Q\,(\sinh(\alpha l) - \sin(\alpha l)) \tag{14}$$

$$P(\sin(\alpha l) + \sinh(\alpha l)) = Q(\cos(\alpha l) - \cosh(\alpha l)) \tag{15}$$

eliminating P and Q,

$$\sinh^2(\alpha l) - \sin^2(\alpha l) = \cos^2(\alpha l) + \cosh^2(\alpha l) - 2\cos(\alpha l)\cosh(\alpha l) \tag{16}$$

remember; $\cosh^2(\alpha l) - \sinh^2(\alpha l) = 1$, then, the equation becomes;

$$1 - \cos(\alpha l)\cosh(\alpha l) = 0 \tag{17}$$

Equation (17) can only be solved by trial and error methods. The values of α are obtained at about 4.73, 7.85 and 10.99 for the 1st, 2nd and 3rd natural frequencies of a beam, respectively. In this case, using (7), the first (fundamental) natural frequency is expressed in radian per second (rad/s) or in Hertz (Hz) shown in (18) and (19), respectively:

$$\omega_1 = (\frac{4.73}{l})^2 \sqrt{\frac{EI}{\rho A}} \quad \text{(rad/s)} \tag{18}$$

$$\text{and, } f_1 = \frac{1}{2\pi}(\frac{4.73}{l})^2 \sqrt{\frac{EI}{\rho A}} \quad \text{(Hz)} \tag{19}$$

It is important to note that the boundary conditions for clamped-free beam ends are: at $x = 0$, $v = dv/dx = 0$, but at $x = l$, $BM = SF = 0$, where dv/dx is the slope of a continuous beam. Thus, when these boundary conditions are applied to the beams with clamped-free ends, all the parameters shown in (18) and (19) remain the same except α values that are dependent upon boundary conditions. In this case, the values of α are about 1.87, 4.69, and 7.85 for the 1st, 2nd and 3rd natural frequencies of a beam with clamped-free ends, respectively. It is worth pointing out that Young's modulus (E) of a beam is dependent upon the natural frequency (f), density (ρ), cross-sectional area (A), the moment of inertia (I), length (l) and α as shown in (19), and that only the first natural frequency of the beams has been used for the measurements. In this case, α values of 4.73 and 1.87 were used for the beams with free-free and clamped-free end conditions, respectively.

B. Damping

For an elastic solid structure, damping is defined as the conversion of mechanical energy into thermal energy, and it is defined in a number of different, yet related ways [19]. In this study, the half-power bandwidth method was used for measuring the damping values, which are determined from the curve of velocity amplitude against frequency, obtained when the specimen is impacted by the hammer. The 'half-power bandwidth' is (f_2-f_1) where f_2 *and* f_1 are the frequencies at which the amplitude falls to $1/\sqrt{2}$ of its maximum value, reached on f_n, the resonant frequency. The loss factor, η is defined as:

$$\eta = \frac{f_2 - f_1}{f_n} \tag{20}$$

For convenience, damping is usually presented in SDC, ψ, which is defined as the ratio between the energy dissipated per cycle and the maximum stored elastic energy per cycle per unit volume [20]. It is usually expressed as a percentage.

For small damping, the relationship between ψ and η is [21],

$$\psi = 2\pi\eta \; x \; 100 \tag{21}$$

IV. Results and Discussion

First, validation of the test was made with respect to the non-contact experimental set-up used in Figs. 3 and 4. For this purpose, the aluminum specimens considered to have well-established data in the literature were subjected to the vibration tests, and their values presented through Figs. 6-8 are evaluated here to interpret the remaining results with confidence. The 2024-T3 aluminum alloy specimens were machined in the form of beams with dimensions of 250 mm in length, 26.10 mm in width and 1.97 mm in thickness, and with a mass of 35.42 gr and a density of 2755.5 kg/m^3. The specimens with free-free ends and also with clamped-free ends were subjected to the vibration tests shown in Figs. 3 and 4, respectively. While the former gave a first natural frequency of about 164.30 Hz and a flexural modulus of about 70.86 GPa, the latter gave a value of about 30.20 Hz and 69.50 GPa. It was found that the elastic modulus (70.86 GPa and 69.50 GPa) obtained is consistent with those obtained from the literature [26]. This gave confidence about the values obtained from the non-contact experimental set-up explained above. On the other hand, the value of SDC was about 0.47% for the specimens with free-free ends, and about 2.2% for those with clamped-free ends. It was found that the latter gave more than 4.6 times greater values compared to the former. These results make the set-up with clamped-free boundary conditions questionable, true, especially for the specimens with relatively low SDC. These values were obtained from the continuous clamping region where there was a constant interaction of fixed support with the specimen's clamped part. For comparison reasons, the tests were also conducted using the clamping region with two-contact points where there were two different points of interactions of the fixed support with the specimen's clamped part (see Fig. 4). In this case, SDC was about 1.98% that was about 10% decrease in the value. However, it was found that the two-contact clamping region could cause some local failure in the specimens due to the concentrated contact loading, therefore, this type of clamping region was not used anymore. Briefly, the remaining results to be discussed will be from the free-free boundary conditions and also from the continuous clamping region.

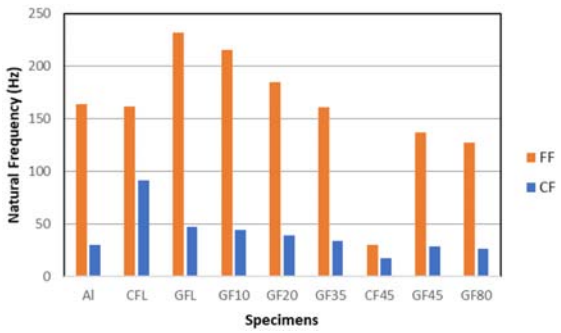

Fig. 6 The experimental first (fundamental) natural frequencies of the specimens with free-free (FF) and clamped-free (CF) boundary conditions

Fig. 6 represents the experimental first (fundamental) natural frequencies of the beams with free-free and clamped-free boundary conditions, respectively. As expected, fiber orientations and the dimensions of the specimens play an important part in the values; while the higher values are from the specimens with low angles of the orientations (i.e., 0° and ± 10°), the lower ones are from those with the higher angles (i.e., ± 45° and 80°). And also, the specimens with relatively short lengths give relatively higher natural frequency values, compared to those with relatively long lengths. In general, the frequency values of the beams with free-free ends are higher than those with clamped-free ends, which is related to (19) and

(20), respectively; while all the parameters affecting the natural frequency are the same, only the eigenvalue (α) for the end conditions are different. While the values of the frequency for the specimens with free-free ends are about 164 Hz, 162 Hz, 231 Hz, 216 Hz, 185 Hz, 61 Hz, 30 Hz, 137 Hz and 127 Hz, those with clamped-free ends are 30 Hz, 92 Hz, 48 Hz, 45 Hz, 39 Hz, 34 Hz, 18 Hz, 29 Hz and 26 Hz, respectively.

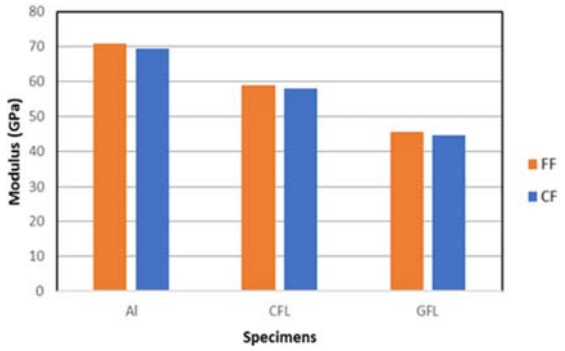

Fig. 7 (a) A comparison of flexural modulus results of category 1 specimens from the free-free (FF) and clamped-free (CF) ends boundary conditions

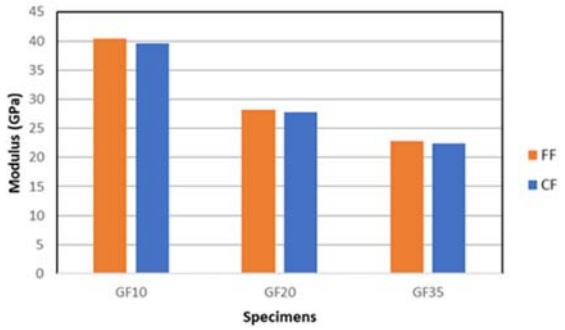

Fig. 7 (b) A comparison of flexural modulus results of category 2 specimens from the free-free (FF) and clamped-free (CF) ends boundary conditions

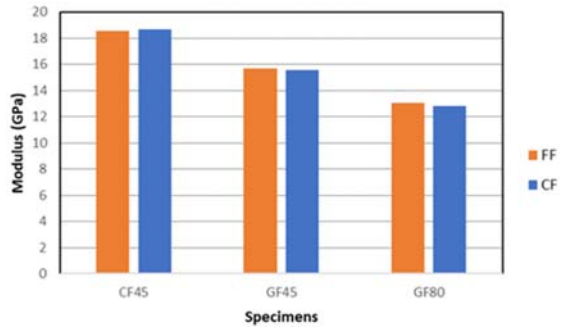

Fig. 7 (c) A comparison of flexural modulus results of category 3 specimens from the free-free (FF) and clamped-free (CF) ends boundary conditions

Through Figs. 7 (a)-(c), a comparison of the flexural modulus values from the beams with the two different end conditions, free-free and clamped-free, can be observed. Overall, the values of modulus are in agreement with respect to their angles of fiber orientations considering the composite specimens. The higher values are obtained from the specimens with the small angles (i.e., 0° and ± 10°), but the lower are from the higher angles (i.e., ± 45° and 80°), a similar tendency to the results of the natural frequency. The modulus values are about 45 GPa, 39 GPa, 28 GPa, 22 GPa, 15 GPa and 14 GPa for the glass fiber-reinforced composite beams with 0°, ± 10°, ± 20°, ± 35°, ± 45° and 80° fiber orientations, respectively. The modulus values for the carbon fiber-reinforced CFL and CF45 specimens are about 59 GPa and 17 GPa, respectively. It is clear that the specimens with free-free and clamped-free ends give consistent results for all the categories (1, 2 and 3) described in Section II *A* and in Fig. 1, and the maximum deviation between both end conditions (free-free and clamped-free) is about 2% for the GF10 specimens. At least four specimens for each type were tested and a variation of less than 1% was obtained in the results that were repeatable fairly enough.

Figs. 8 (a)-(c) show a comparison of the SDC values of the specimens with free-free and clamped-free ends. The values of the specimens in category1 that is Al, CFL and GFL are about 0.47%, 1.17% and 1.25%, respectively, from the free-free ends boundary conditions. The values from the same specimens with clamped-free ends are about 2.2%, 2.12% and 1.98%, respectively (see Fig. 8 (a)). The difference in the values of the specimens in the category1 is quite large, and the latter end conditions give quite high values of SDC. The increase in the damping values is about 368%, 81% and 58% in comparison with the former end conditions for the Al, CFL and GFL specimens, respectively.

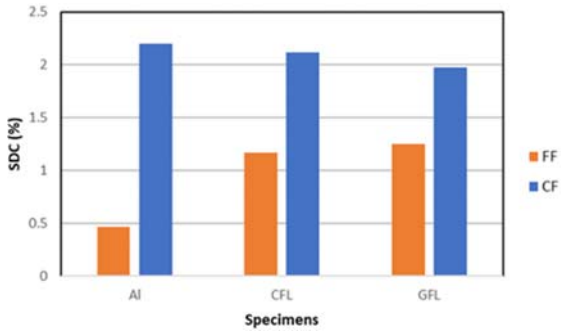

Fig. 8 (a) A comparison of SDC results of category 1 specimens from the free-free (FF) and clamped-free (CF) ends boundary conditions

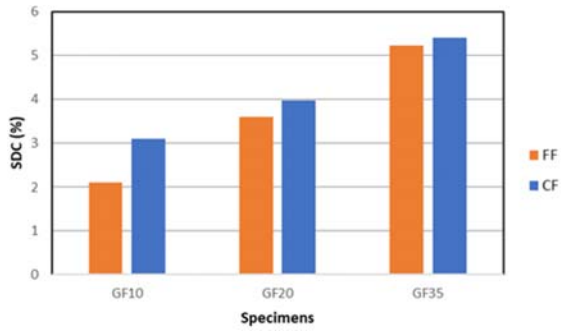

Fig. 8 (b) A comparison of SDC results of category 2 specimens from the free-free (FF) and clamped-free (CF) ends boundary conditions

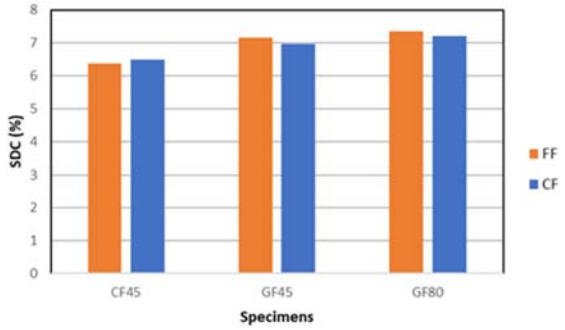

Fig. 8 (c) A comparison of SDC results of category 3 specimens from the free-free (FF) and clamped-free (CF) ends boundary conditions

From Fig. 8 (b), it is seen that the difference in the damping value of the specimens in category2 (GF10, GF20 and GF35) is not much, although those with clamped-free ends are relatively high, again. While the values of those with free-free ends are about 2.11%, 3.60% and 5.23%, those with clamped-free ends have about 3.1%, 3.98% and 5.4%. The difference in the SDC is about 47%, 11% and 3%, respectively. It is important to note that as inherent damping values increase the difference between both end conditions (free-free and clamped-free) decreases. This can be seen clearly in Fig. 8 (c) which is for the specimens for category3 (CF45, GF45 and GF80). The values of the SDC are about 6.4% and 7% and 7.3%, respectively. The maximum difference between the values from both boundary conditions is only about 2% which is the GF45 specimen. It is clear that all the results in category3 are comparable and that the difference can be ignored.

The formulations for the beams with free-free and clamped-free end conditions have been found successfully which are presented in (18) and (19), respectively. The formulas have been validated through the experimental set-ups shown in Figs. 3 and 4 that are able to vibrate the specimens via an induced air flow, a non-contact exciting mechanism. The measuring instrument selected to pick up the response from the vibrating beam has also a non-contact feature, a laser head. It is believed that a correct (reliable) damping measurement of structures is possible to obtain in this way because such a set-up is able to isolate the specimen under the test from its surrounding as much as possible. It is seen from Fig. 8 (a) that the damping values are sensitive to the end conditions if the inherent value of a structure is low. For instance, the SDC values of the specimens in category1 deviate nearly 368%, 81% and 58% for Al, CFL and GFL, respectively, if the free-free ends are compared with clamped-free ends. Here, the fixed (clamped) part of the specimen creates some extraneous damping values that make the specimens with the low damping values questionable if the clamped ends are to be used. Although not as much as the specimens in the category1, the deviation is still the case for the composite beams in the category2 whose basic properties are controlled mainly by the glass fibers, ± 10°, ± 20° and ± 35°. It is well known that the specimens controlled by the mechanical properties of the fiber constituents have relatively high strength but low damping values, which is opposite to those controlled by the matrix constituent which presents high damping but low strength values. In line with this context, the experimental set-up with the free-free end conditions is able to provide reliable values for the specimens with 0°, ± 10°, ± 20° and ± 35° fiber orientations compared to those with the ± 45° and 80° orientations that are controlled by the properties of the matrix. This is also true for the CFL and CF45 specimens. It is believed that the experimental set-up with clamped-free end conditions is not able to produce reliable damping data, especially for the high-strength metals, too, as the current work has proven the deviation between the two end conditions (free-free and clamped-free) is too large that 368% for the aluminum (Al) specimens. On the other hand, there is no superiority of the free-free ends as it gives consistent results with the specimens with the clamped-free ends. In overall, it is fair to claim that the specimens with high inherent damping values, say more than 6% SDC, can be subjected to the vibrating beam technique with either free-free or clamped-free end conditions as they both produce comparable and reliable damping data. However, as the inherent damping values of structures are getting lower, the sensitivity of these values to the boundary conditions is getting large, especially the case for the specimens in the category1.

In spite of the effects of the boundary conditions on the damping values of the specimen beams, the results of flexural modulus are presented in Figs. 7 (a)-(c) do not seem to be affected by the boundary conditions considerably. The maximum difference between the two test set-ups is about 2% for the different categories of specimens. For example, the value of the modulus for the aluminum specimens is about 70 GPa for both end conditions, in spite of a large difference in the damping values.

It is important to note that any exciting and/or response measuring devices such as accelerometers, strain gauges, etc. attached to the specimens under the vibration test are likely to affect their dynamic (damping and elastic modulus) results leading to much more complex calculations as the existence of the each attached device introduces an extraneous mass on the specimens. Contrary to this, the experimental setups presented in Figs. 3 and 4 allow a straightforward calculation of the dynamic values of each specimen under the test.

V. Conclusions

Correct dynamic values of advanced materials such as polymer composites are vital for their reliable designs as they are mainly used in today's modern aircraft and automobiles. It is well known that the inherent damping of these materials helps avoid excessive vibrations and so provides comfort and good acoustic properties for passengers, and also increases the fatigue life of the components. The correct damping values are mainly based on the excitement and picking up measuring devices and also boundary conditions, as the case for the current study. It has been proved that the damping values of the composite specimens with low angles of fiber orientations are sensitive to the boundary conditions, namely, the differences in the values of the SDC of the specimens with the free-free and clamped-free ends are about 60%, 47%, 11%, and 3% for the orientations of 0°, ± 10°, ± 20° and ± 35°, respectively. On the

other hand, this difference can be ignored for those with higher angles of fiber orientations. It is clear that the experimental setup with the clamped-free boundary conditions is not suitable for reliable damping measurements of the specimens possessing low structural damping values, while that with the free-free ends is a reliable technique for collecting such data.

ACKNOWLEDGMENT

We would like to thank the Turkish Aerospace Industry (TAI) for providing the specimens.

REFERENCES

[1] S. Prabhakaran, V. Krishnaraj, M.S. Kumar, R. Zitoune, Sound and vibration damping properties of flax fiber reinforced composites, Procedia Eng. 97 (2014) 573 – 581.
[2] J.J. Sargianis, H.I. Kim, E. Andres, J. Suhr, Sound and vibration damping characteristics in natural material based sandwich composites, Compos. Struct. 96 (2013) 538–544.
[3] P. Jeyaraj, N. Ganesan, C. Padmanabhan, Vibration and acoustic response of a composite plate with inherent material damping in a thermal environment, J. Sound Vib. 320(1) (2009) 322–338.
[4] P. Jeyaraj, C. Padmanabhan, N. Ganesan, Vibro-acoustic behavior of a multilayered viscoelastic sandwich plate under a thermal environment, J. Sandw. Struct. Mater. (2011) 1099636211400129.
[5] M.P. Arunkumar, M. Jagadeesh, J. Pitchaimani, K.V. Gangadharan, M.C.L. Babu, Sound radiation and transmission loss characteristics of a honeycomb sandwich panel with composite facings: effect of inherent material damping, J. Sound Vib. 383 (2016) 221–232.
[6] G. Petrone, V.D. Alessandro, F. Franco, S. DeRosa, Numerical and experimental investigations on the acoustic power radiated by aluminum foam sandwich panels, Compos. Struct. 118 (2014) 170–177.
[7] G. Petrone, S. Rao, S. DeRosa, B. Mace, F. Franco, D. Bhattacharyya, Initial experimental investigations on natural fiber reinforced honeycomb core panels, Compos. B Eng. 55 (2013) 400–406.
[8] Z. Zhang, G. Hartwig, Relation of damping and fatigue damage of unidirectional fiber composites, Int. J. Fatigue. 24 (2002) 713-718.
[9] A.L. Audenino, V. Crupi, E.M. Zanetti, Correlation between thermography and internal damping in metals. Int. J. Fatigue. 25 (2003) 343-351.
[10] L. Thomas, L.H. Attard, Z. Hongyu, Improving damping property of carbon-fiber reinforced epoxy composite through novel hybrid epoxy-polyurea interfacial reaction, Compos. B Eng. 164 (2019) 720–731.
[11] M. Rafiee, F. Nitzsche, M.R. Labrosse, Effect of functionalization of carbon nanotubes on vibration and damping characteristics of epoxy nanocomposites, Polym. Test. 69 (2018) 385–395.
[12] A. Monti, A. El Mahi, Z. Jendli, L. Guillaumat, Experimental and finite elements analysis of the vibration behavior of a bio-based composite sandwich beam, Compos. B Eng. 110 (2017) 466-475.
[13] J. Sargianis, J. Suhr, Effect of core thickness on wave number and damping properties in sandwich composites, Compos. Sci. Technol. 72(6) (2012) 724–730.
[14] E.P. Bowyer, V.V. Krylov, Experimental investigation of damping flexural vibrations in glass fibre composite plates containing one- and two-dimensional acoustic black holes, Compo. Struct. 107 (2014) 406–415.
[15] M.P. Arunkumar, J. Pitchaimani, K.V. Gangadharan, M.C. Leninbabu, Vibro-acoustic response and sound transmission loss characteristics of truss core sandwich panel filled with foam, Aerosp. Sci. Technol. 78 (2018) 1–11.
[16] S.U. Khan, C.Y. Li, N.A. Siddiqui, J.K. Kim, Vibration damping characteristics of carbon fiber-reinforced composites containing multi-walled carbon nanotubes, Compos. Sci. Technol. 71 (2011) 1486–1494.
[17] S.K. Bhudolia, P. Perrotey, S.C. Joshi, Enhanced vibration damping and dynamic mechanical characteristics of composites with novel pseudo-thermoset matrix system, Compos. Struct. 179 (2017) 502–513.
[18] M. Rueppel, J. Rion, C. Dransfeld, C. Fischer, K. Masania, Damping of carbon fibre and flax fiber angle-ply composite laminates. Compos. Sci. Technol. 146 (2017) 1-9.
[19] Y. Li, S. Cai, X. Huang, Multi-scaled enhancement of damping property for carbon fiber reinforced composites, Compos. Sci. Technol. 146 (2017) 1-9
[20] H. Dewa, Y. Okada, B. Nagai, Damping characteristics of flexural vibration for partially covered beams with constrained viscoelastic layers, JSME Int. J. Ser. III. 34(2) (1991) 210–217.
[21] M.D. Rao, M.J. Crocker, Vibrations of bonded beams with a single lap adhesive joint, J. Sound Vib. 92(2) (1990) 299–309.
[22] T.H. Park, Vibration and damping characteristics of a beam with a partially sandwiched viscoelastic layer, J. Adhes. 61(1–4) (1997) 97–122.
[23] B.E. Douglas, J.C.S. Yang, Transverse Compressional damping in the vibratory response of elastic–viscoelastic beams, AIAA J. 16(9) (1978) 925–930.
[24] G.L. Qian, S.V. Hoa, X. Xiao, A vibration method for measuring mechanical properties of composite, theory and experiment, Compos. Struct. 39 (1997) 31–38.
[25] F.J. Guild, R. D. Adams, A new technique for the measurement of the specific damping capacity of beam in flexure, J. Physics E: Sci. Instrum. 14 (1981) 355–363.
[26] J.E. Shigley, C.R. Mischke, Mechanical engineering design, (1986) 5th ed. New York, McGraw-Hill.

F. Kadioglu earned his Doctor of Philosophy degree from the University of Bristol between 1996-2000. He wrote a thesis on the quasi-static and dynamic behavior of a structural pressure-sensitive adhesive.

He is an academician as a Professor Doctor in the Department of Aerospace Engineering at Ankara Yıldırım Beyazıt University. He has many publications such as Damping Contribution of the Glass Reinforced Aluminum Laminates Epoxy to the Aluminum-Basedsandwich Structures[1] and Mechanical Behaviour of Adhesively Single Lap Joint Under Buckling Conditions[2]. His research interests are as follows: Solid mechanics, fracture mechanics, mechanical tests, material technologies, and test techniques.

1. Damping Contribution of the Glass Reinforced Aluminum Laminates Epoxy to the Aluminum-Basedsandwich Structures (Ankara: F. Kadioglu, 2022)
2. Mechanical Behaviour of Adhesively Single Lap Joint Under Buckling Conditions (Ankara: F. Kadioglu, 2021)

M. Z. Polat works as a Research Assistant at Yıldırım Beyazıt University and continues his master's degree. Between 2018 and 2019, he worked as a candidate engineer in the Turkish Aerospace Industry.

A.R. Gunay was born in Ankara in 1984. He graduated from the Kırıkkale University Civil Engineering program in 2006. Between 2008 and 2011, he completed his master's degree at Istanbul Technical University Structural Engineering Department. In 2021, he received his Doctor of Philosophy degree in Mechanical Engineering from Baskent University.

He worked at TUBITAK Marmara Research Institute between 2007 and 2012. He is still working as a division manager in the construction, and maintenance operation unit of the TUBITAK Defense Industry Research and Development Institute, which he entered in 2012. He also works as a part-time employee at Atılım University. He has a publication name is An Experimental Study on the Dynamic Behavior of Ultra High Strength Concrete.[3]His research interests are as follows: Concrete and steel materials, impact mechanics, fragmentation, blast effect, dynamic loading.

1. An Experimental Study on the Dynamic Behavior of an Ultra High-Strength Concrete (Ankara: A.R. Gunay, S. Karadeniz, M. Kaya, 2020)